SCIENCE APPLICATIONS, INC.

THREE-DIMENSIONAL COMPUTER MODEL
FOR THE ATMOSPHERIC GENERAL
CIRCULATION EXPERIMENT

SAI-84/1142

**SCIENCE APPLICATIONS, INC.**

Post Office Box 1303, 1710 Goodridge Drive, McLean, Virginia 22102, (703) 821-4300

# THREE-DIMENSIONAL COMPUTER MODEL FOR THE ATMOSPHERIC GENERAL CIRCULATION EXPERIMENT

SAI-84/1142

June 1984

Prepared by:

Glyn O. Roberts

Prepared for:

Marshall Space Flight Center
National Aeronautics and Space Administration

Final Report on
Contract NAS8-34751

SCIENCE APPLICATIONS, INC.

1710 Goodridge Drive
P. O. Box 1303
McLean, VA 22102
(703) 821-4300

Science Applications, Inc.

TABLE OF CONTENTS

TABLE OF CONTENTS (cont.)

LIST OF FIGURES

## LIST OF TABLES

## SUMMARY

We are developing an efficient, flexible, three-dimensional, hydrodynamic, computer code for a spherical cap geometry. The code will be used to simulate NASA's Atmospheric General Circulation Experiment (AGCE). The AGCE is a spherical, baroclinic experiment which will model the large-scale dynamics of our atmosphere; it has been proposed to NASA for future Spacelab flights. In the AGCE a radial dielectric body force will simulate gravity, with hot fluid tending to move outwards. In order that this force be dominant, the AGCE must be operated in a low gravity environment such as Spacelab.

The full potential of the AGCE will only be realized by working in conjunction with an accurate computer model. Proposed experimental parameter settings will be checked first using model runs. Then actual experimental results will be compared with the model predictions. This interaction between experiment and theory will be very valuable in determining the nature of the AGCE flows and hence their relationship to analytical theories and actual atmospheric dynamics.

Although much is understood about the averaged steady-state behavior of our atmosphere, most of the time-dependent activity is still unexplained. We expect, from previous experimental work with cyclindrical baroclinic laboratory models, that the AGCE will also exhibit many periodic and irregular flows. It is the major thrust of the AGCE program to analyze these strongly nonlinear, unsteady flows.

The computer model is based on the complete set of fully nonlinear, incompressible equations. Previous computer codes are inadequate for the accurate simulations required. It is known, from theory, axisymmetric computations and the cylindrical experiments, that the AGCE type flows have thin thermal layers and plumes. This necessitates nonuniform finite-difference meshes, and makes the hydrostatic assumption a questionable approximation. Further, the wide range of flow types and parameters, and the resulting large number of cases, imply a requirement for efficient state-of-the-art coding, with implicit methods, able to utilize the new fifth-generation vector processors.

The model is being made flexible so that it can be used for design studies for other possible future spherical Spacelab experiments dealing with the oceans or other planetary atmospheres, and for studies in cylindrical geometry. The model will be properly validated using available accurate flow measurements.

The development, testing and application of this code is a substantial task. We originally proposed to develop this three-dimensional code in 1981, in a three year program. Funding constraints have so far allowed us to perform only about 40% of the work, in the first two years. We estimate that it will take a further three years to complete. During the third year the code and diagnostics will be completed and tested, and cylindrical validations will be performed. During the fourth year spherical validations will be performed, with timing and convergence tests. During the fifth year we will model a variety of proposed AGCE configurations and tests.

# Section 1
# BACKGROUND

## 1.1 THE CYLINDRICAL ANNULUS FLOWS

One of the major unsolved problems of meteorology is the persistence and irregularity of our atmosphere. Although the mean steady general circulation is quite well understood, the time-dependent behavior is not. The large-scale atmospheric flow sometimes forms a relatively stable pattern that persists for many days or weeks, while at other times it is much more transitory.

A fundamental attack on these problems has been made through the study of well-defined laboratory model flows. In particular, since the 1950's a substantial amount of experimental work has been devoted to the study of baroclinic flows in a rotating and differentially heated cylindrical annulus of liquid (References 1 through 5). Systematic scaling of the governing equations for both our atmosphere and the cylindrical annulus reveals that the annulus is a model of the large-scale (synoptic) atmosphere flow (Reference 6). As the parameters in the experiment are varied, axisymmetric flows, steady wave flows, periodically fluctuating wave flows (vacillations) and irregular flows are observed. Figure 1 is a schematic diagram of the cylindrical annulus, Figure 2 shows a typical wave flow and Figure 3 is a flow regime diagram.

Analytical studies have contributed to an understanding of these baroclinic flows, but owing to the mathematical difficulties associated with cylindrical geometry,

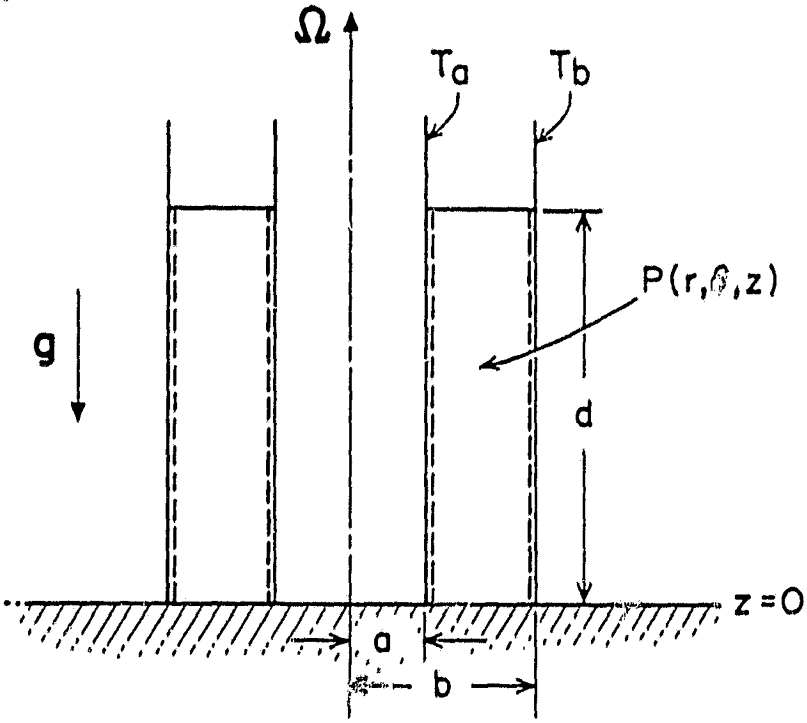


| | | |
|---|---|---|
| P | - | General point having cylindrical polar coordinates $(r,\theta,z)$ in frame rotating with the apparatus |
| $\boldsymbol{\Omega}$ | $= (0,0,\Omega)$ - | rotation vector |
| $\mathbf{g}$ | $= (0,0,-g)$ - | acceleration of gravity |
| b, a, d | - | fluid occupies region $a < r < b,\ 0 < z < d\left[1+\Omega^2(r^2 - 1/2(b^2+a^2))/2gd\right] \simeq d$ |
| $T(r,\theta,z,t)$ | - | temperature at general point P and time t |
| $T_a, T_b$ | - | $T(a,\theta,z,t)$; $T(b,\theta,z,t)$ respectively |

Figure 1 Schematic Diagram Illustrating Rotating Fluid Annulus

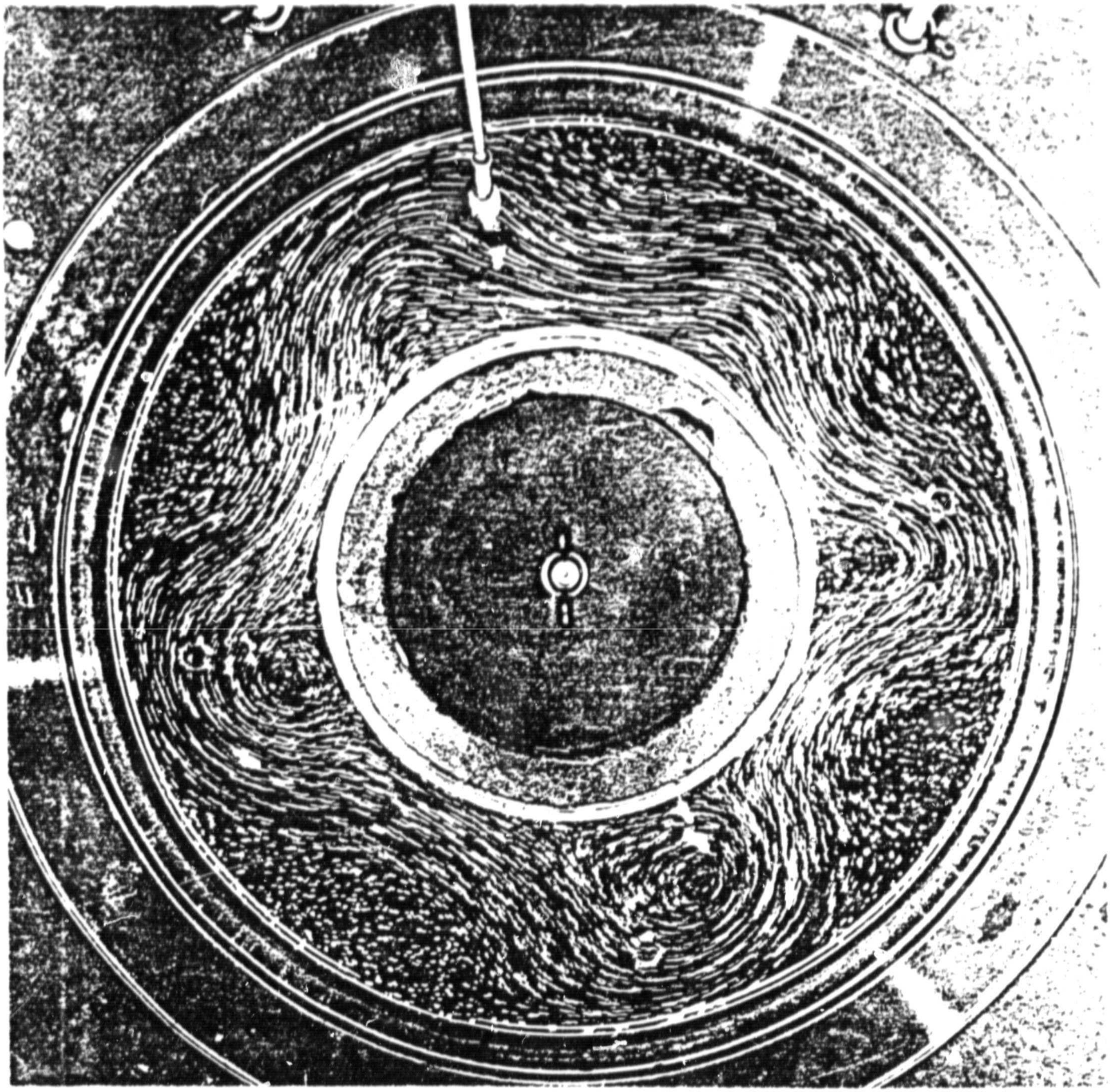

Figure 2  Photograph of a Typical Annulus Wave Flow

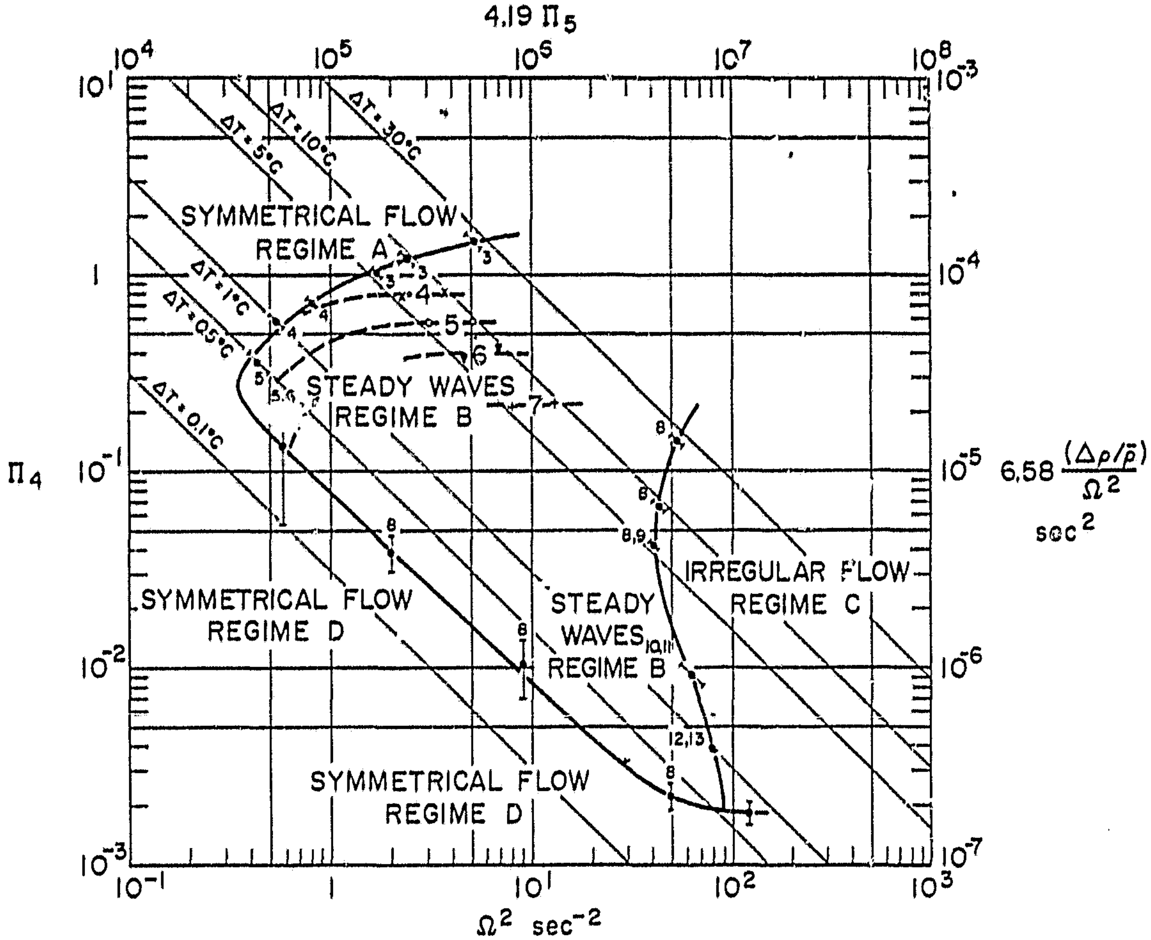


$$\Pi_4 = \frac{gd(\Delta\rho/\bar{\rho})}{\Omega^2(b-a)^2} \quad , \quad \Pi_5 = \frac{4\Omega^2(b-a)^5}{\bar{\nu}^2 d} \quad , \quad \Pi_6 = \frac{\bar{\nu}}{\bar{\kappa}} \quad .$$

Figure 3 Experimental results on the transitions between the flow regimes and wave numbers for a fixed depth of water in the annulus and for fixed radii of the cylinders, plotted in the $\pi_4$ versus $\Omega^2$ diagram. Experimental details: a = 3.48cm, b = 6.02cm, d = 10.00cm, T = 20.0°C, $\bar{\nu}$ = 1.01 x $10^{-2}$cm$^2$sec$^{-1}$, $\bar{\rho}$ = 0.998gm cm$^{-3}$, $\pi_6$ = 7.19.

non-separability and nonlinearity, these studies have dealt mainly with simplified models and linearized stability problems (References 7, 8 and 9). Numerical studies have dealt with the basic axisymmetric states and with a steady wave flow (References 10, 11 and 12). Much has been learned from the annulus work about baroclinic instability and baroclinic waves, and insight into the behavior of large-scale atmospheric dynamics has been achieved (References 13 and 14).

## 1.2 THE AGCE

The major inadequacy of the cylindrical annulus configuration as a model of the atmosphere is the absence of spherical curvature. A true spherical model requires a radial gravity field.

In 1978, a proposal for a spherical baroclinic experiment known as the Atmospheric General Circulation Experiment (AGCE) was submitted to the Global Weather Program, NASA/OSSA. In the apparatus proposed, the liquid is held between two concentric spheres, with a large AC voltage applied across them. The resulting temperature-dependent dielectric body force corresponds exactly to the inward gravity acceleration,

$$g_E = \frac{2\varepsilon\gamma V^2}{\rho\alpha} \left\{\frac{r_t r_b}{r_t - r_b}\right\}^2 r^{-5} \qquad (1)$$

Here $\varepsilon$ and $\rho$ are the dielectric constant and the density, $\gamma$ and $\alpha$ are the corresponding thermal coefficients, $r_b$ and $r_t$ are the inner and outer radii, $V$ is the voltage and $r$ is the radius. In order for $g_E$ to be dominant the AGCE apparatus will have to be flown in an orbiting vehicle such as Spacelab. Figure 4 is a schematic drawing of a proposed apparatus. This figure also includes some preliminary estimates for the dimensions and imposed conditions. Temperatures are maintained on the spherical boundaries such that the liquid experiences a stable radial gradient and a latitudinal gradient. The spheres are rigidly corotated. Scientific and engineering design studies for the AGCE are under way.

Substantial differences between the AGCE flows and the cylindrical annulus flows are anticipated. It is the major objective of the AGCE program to study the non-linear unsteady flows occurring in the spherical model.

Another spherical geophysical fluid dynamics experiment which also exploits the radial dielectric body force was proposed earlier than the AGCE and will be flown on Spacelab 3. This experiment is known as the Geophysical Fluid Flow Cell (GFFC) and is concerned with convection due to radially unstable temperature gradients. The scientific teams for the AGCE and the GFFC are listed in Table 1.

## 1.3 The AGCE DESIGN PROGRAM

The major objective of the AGCE is to study non-linear, baroclinic wave flows in a spherical geometry. Thus the experiment must allow a parameter range in which axisymmetric flows are strongly baroclinically unstable. A number of preliminary analytical design study calculations for the AGCE have been performed and the results indicate that to

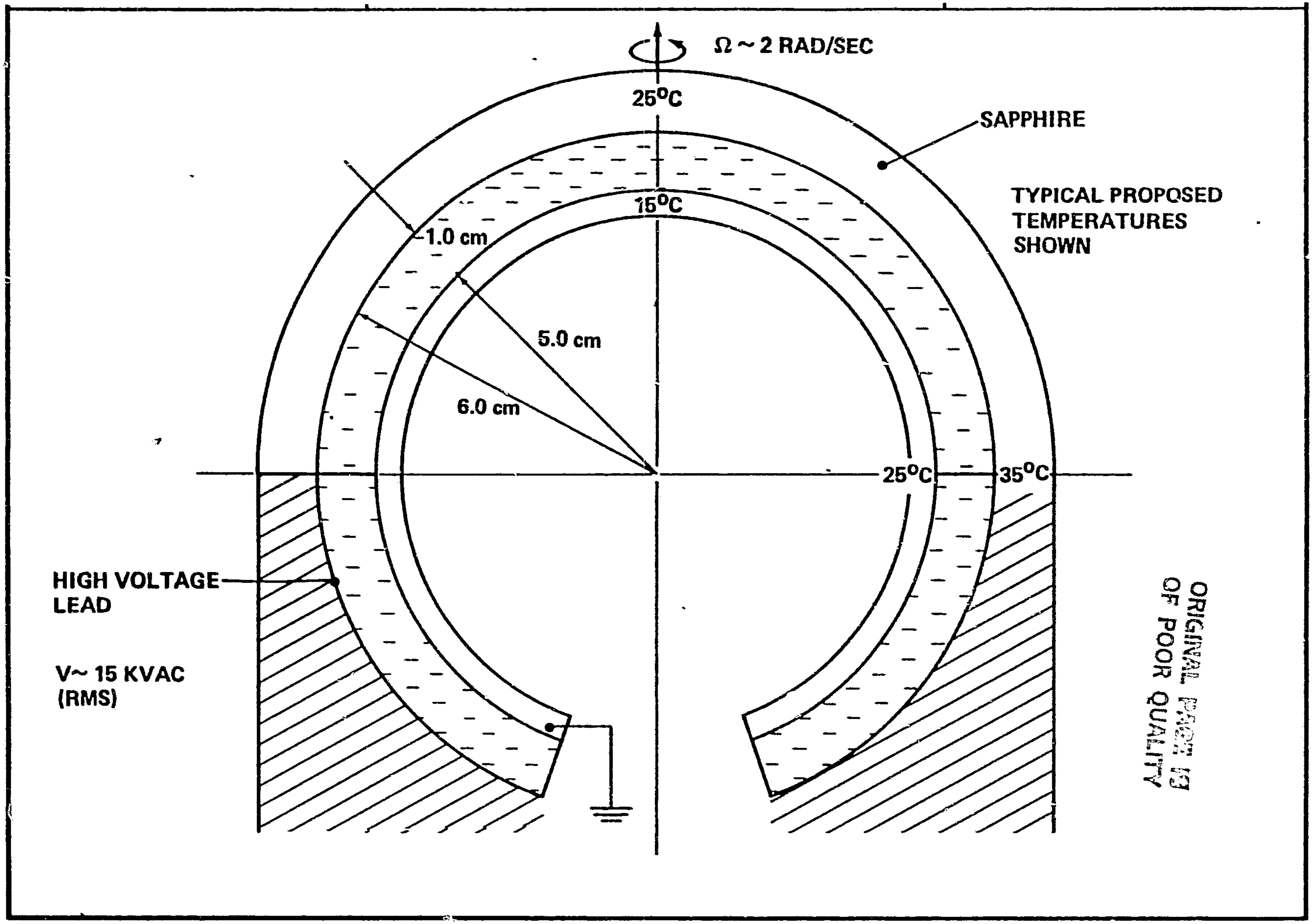


ORIGINAL PAGE IS
OF POOR QUALITY

Figure 4  Schematic Drawing of the Proposed AGCE Apparatus

Table 1

SCIENTIFIC TEAMS FOR SPACELAB EXPERIMENTS

Geophysical Fluid Flow Cell (GFFC)

| | |
|---|---|
| Principal Investigator: | John Hart (Univ. of Colorado) |
| Co-investigators: | Juri Toomre (Univ. of Colorado) |
| | Peter Gilman (NCAR/HAO) |
| | George Fichtl (NASA/MSFC) |
| | William Fowlis (NASA/MSFC) |
| | Fred Leslie (NASA/MSIC) |

Atmospheric General Circulation Experiment (AGCE)

| | |
|---|---|
| Principal Investigator: | William Fowlis (NASA/MSFC) |
| Co-investigators: | George Fichtl (NASA/MSFC) |
| | John Geisler (Univ. of Utah) |
| | Robert Gall (Univ. of Arizona) |
| | Basil Antar (Univ. of Tennessee Space Institute) |
| | Glyn Roberts (SAI) |
| | Eric Pitcher (Univ. of Miami) |
| | Timothy Miller (NASA/MSFC) |

obtain strong instability the apparatus will have to be carefully designed (References 15 through 23). However, because of the simplifications which have to be made to perform analytical calculations, these results must be considered qualitative in nature and cannot be used to prepare specifications for the apparatus. For quantitative theoretical work, numerical models are required.

## 1.4 THE AXISYMMETRIC AND STABILITY CODES

A numerical modeling design program for the AGCE is under way (References 31 through 34). The approach taken was to develop two numerical models. The first model obtains steady, axisymmetric basic states for the spherical geometry and is based on the complete, fully nonlinear set of equations. The second model examines the stability of these basic states. It is based on the complete linearized set of pertubation equations. We are running these two-dimensional models for systematically varied values of the AGCE dimensions, fluid properties and imposed conditions. This work is producing theoretical regime diagrams comparable to Figure 3, which can be used to prepare specifications for the AGCE apparatus such that strong baroclinic instability will be achieved.

We validated these models by applying them to a cylindrical geometry. Experimental and numerical data are available for the basic states of the cylindrical annulus flows, and experimental data are available for the regime diagrams (References 3, 4, 10, 11, 12, 24 and 25). Excellent agreement has been obtained. We have also compared the predictions of the stability code with the experimental regime diagrams. Again, the agreement was excellent. Finally, we validated the spherical basic state model using laser-Doppler measurements of spin-up in spherical geometry (cf., Reference 26).

# Section 2
# THREE-DIMENSIONAL NUMERICAL MODEL FOR THE AGCE

## 2.1 MODEL OBJECTIVES AND JUSTIFICATION

Although a substantial amount of work with two-dimensional numerical models is under way (see Section 1.4), the full scientific potential of the AGCE will not be realized unless a three-dimensional, fully nonlinear, numerical model based on the complete set of equations is also available. We are developing such a model.

The model has two primary objectives. First, it will demonstrate the possible types of nonlinear baroclinic wave flows that may occur in AGCE for different parameter ranges. This will aid in the selection of the sequence of experimental parameters for the AGCE on Spacelab. Secondly, the numerical results will extend the limited measurements that can be made with the AGCE apparatus. Owing to the relatively small and confined volume of fluid and to the presence of the large AC electric field, it will not be possible to measure the fluid behavior thoroughly. Techniques for flow and temperature measurement for the AGCE have been proposed (References 15 and 27). If the measurements agree with the model predictions, this will tend to confirm both the model predictions of the whole flow and temperature field, and also the model predictions for other cases.

## 2.2 SPECIFICATION OF THE PROBLEM

### 2.2.1 Model Equations

We are using the Boussinesq convection equations in the spherical polar coordinates $(\theta,\lambda,r)$, with corresponding velocity components u, v and w. Significant components of our system of equations are summarized in Table 2. The divergence of the stress and momentum tensor has many extra terms associated with the curvilinear coordinate system; these are handled correctly.

The gravity potential $\Phi$ has up to three components, as shown in Tables 2 and 3. The radial component corresponds to an inward gravity field $G_t(r/r_t)^p$; the radial powers of particular interest are -2 for atmospheric gravity and -5 for the gravity field which models the effect of the dielectric body force, cf., Equation (1).

Axial (terrestrial) gravity is included for simulating laboratory experiments in a cylindrical annulus and in prototype AGCE configurations. Centrifugal gravity is included since theory and annulus experiments both demonstrate that it is very significant for the larger rotation rates. It is absent in the atmosphere, since the vertical coordinate is based on equipotential surfaces with the centrifugal potential included.

### 2.2.2 Computational Domain and Special Cases

The axisymmetric computational domain in spherical polar coordinates is defined by the inequalities

Table 2

EQUATIONS FOR THE MODEL

| Component | Description |
|---|---|
| Continuity | Incompressible |
| Formulation | Primitive variable, not hydrostatic |
| Primary variables | $T$, $u$, $v$, $w$, $p$ |
| Thermal Diffusivity | $\kappa$ constant |
| Kinematic viscosity | $\nu$ constant |
| Buoyancy acceleration | $b\nabla\Phi$ |
| Specific volume increase | $b = \alpha T + \alpha_2 T^2$ |
| Heat equation | Optional internal sources or sinks |
| Coriolis force | Coordinates rotate at $\Omega$ |
| Gravity | Radial, axial and centrifugal |

Table 3

GRAVITY POTENTIAL COMPONENTS

| Component | Formulation |
|---|---|
| Radial | $g_t r^{p+1}/(p+1)r_t^{\,p}$ |
| Terrestrial | $gz$ |
| Centrifugal | $-\Omega^2\rho^2/2$ |

$$\theta_\ell < \theta < \theta_r,$$

$$r_b < r < r_t,$$

and shown in Figure 5.

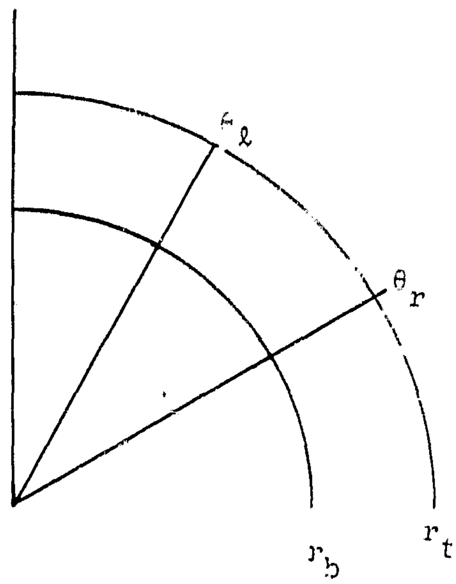


Figure 5  General Form of the Axisymmetric Domain

Special cases of particular interest are listed in Table 4. The extensive set of cylindrical annulus experimental results will provide an important means of code validation. The annulus

$$\rho_\ell < \rho < \rho_r ,$$

$$0 < z < h ,$$

Table 4

SPECIAL CASES FOR THE COMPUTATIONAL DOMAIN

| Case | Values |
|---|---|
| Spherical layer | $\theta_\ell = 0$ , $\theta_r =$ |
| Hemisphere Cap | $\theta_\ell = 0$ , $\theta_r = /2$ |
| Cylindrical Annulus | $\theta_\ell = \rho_\ell/R$ , $\theta_r = \rho_r/R$ |
| | $r_b = R$ $r_t = R + h$ |

can be approximated by using a large value of R. An intermediate value of $\theta_r$ is required for the spherical layer of Figure 4.

### 2.2.3 Options for the Boundary Conditions

There are two basic options for the temperature boundary conditions on each of the four boundary segments,

$$T = \text{imposed distribution, or}$$
$$\partial_n T = 0$$

The second option is appropriate for a thermally insulating boundary. Naturally, at least one boundary must have an imposed temperature distribution.

The four imposed boundary temperature distributions are determined by interpolation from imposed corner temperatures, $T_{b\ell}$, $T_{br}$, $T_{t\ell}$, and $T_{tr}$. Possible values are 15°C, 25°C, 25°C and 35°C. The top and bottom temperatures are linear in an imposed power of $\theta$, in $\cos \theta/\alpha$ or in $\ln(\tan \theta/2)$, at the user's option. The side temperatures are linear in an imposed power of $r$. Other options could easily be added later as the need develops. Examples are to impose the normal heat flux, or to impose the heat flux as a function of the local temperature.

There are four options for the flow boundary conditions on each of the four boundary segments. The first is the no-slip condition, with the solid boundary rotating, relative to the rotating coordinate system, at $\Omega_S - \Omega$. The second is the free-slip condition appropriate to a free surface (and to the equator if it is a symmetry boundary). The third is the axis condition. These three options are summarized in Table 5. The fourth simulates an unresolved turbulent sublayer by making the stress linear in the slip velocity; this option is intended for atmosphere simulations.

Table 5
VELOCITY BOUNDARY CONDITION OPTIONS

| Boundary Type | Boundary Conditions | Location |
|---|---|---|
| No-slip | $u = w = 0$<br>$v = (\Omega_s - \Omega) r \sin\theta$ | All |
| Free-slip | $u = \partial_\theta v = \partial_\theta w = 0$ | $\theta_\ell$, $\theta_r$ |
| | $w = \partial_r v = \partial_r u = 0$ | $r_b$, $r_t$ |
| Axis | $u = v = \partial_\theta w = 0$ | $\theta_\ell = 0$<br>$\theta_r = \pi$ |

### 2.2.4 The $\lambda$ Boundaries

We assume periodicity in the $\lambda$ direction, with period $2\pi/m_\lambda$. This is naturally always valid with $m_\lambda = 1$. By using larger values we can obtain higher resolution at much lower cost.

## 2.3 SPATIAL REPRESENTATION

We use second order finite differences on nonuniform meshes to represent the $\theta$ and r derivatives, as in the present two-dimensional codes (References 31 through 34). We presently use finite differences for the $\lambda$ derivatives: we have not used the attractive fast Fourier transform algorithm because of its poor vectorization properties on the Cyber 205. However, we have written the code in such a way that the Fast Fourier Transform option could be added at a later stage.

### 2.3.1 The Nonuniform Meshes

The mesh spacings for the $\theta$ and r meshes are proportional to the product of the distances from points just outside the domain. This gives small spacings in the boundary layers without wasting mesh points in the interiors. Our $\lambda$ mesh is uniform.

### 2.3.2 Placement of the Variables

We use a staggered computational mesh. The primary variables (T and p) are collocated, and are not defined on the boundary but on points half a mesh interval inside and outside. The velocity components u, v and w are defined at the natural locations for representing the corresponding components of the pressure gradient as differences of adjacent pressure values. This staggered placement of the variables requires averaging in the representation of the Coriolis and buoyancy forces, and slightly increases the total amount of spatial averaging required in the model. However, it gives improved accuracy in the representation of the pressure gradient and the velocity divergence, and makes the pressure equation (a Poisson representation) much more simple than with the non-staggered mesh in our original proposal.

### 2.3.3 Conservation Properties

Our spatial representation conserves representations of total heat and angular momentum, and conserves representations of the $T^2$ and kinetic energy integrals under the action of the advection, Coriolis force, and pressure gradient terms. These are all desirable properties for any spatial representation of these equations, since they help ensure stability and aid in the diagnostics and interpretation.

## 2.4 TEMPORAL REPRESENTATION

### 2.4.1 Time-Stepping and Iterating to a Steady Solution

The code has two objectives and two corresponding modes of operation. One is to determine the detailed time evolution by ordinary time stepping. The other is to iterate to a steady solution. In the second case, we use an iteration method developed for our two-dimensional AGCE studies

(References 31-34) in which the time steps can be different for each mesh point, and different for temperature and velocity. Thus large steps can be taken in the interior, while smaller steps are taken near the boundary where the mesh spacing is smaller.

### 2.4.2 Alternating Direction Implicit Algorithm

We use an ADI treatment for advection, diffusion and Coriolis effects. This allows large time steps, which is a very important consideration in a three-dimensional code. These algorithms were also used in the two-dimensional AGCE studies and in the earlier three-dimensional ocean forecasting code (References 31-36).

### 2.4.3 Internal Waves

We use a leapfrog representation of internal gravity waves, so that the temperature and velocity fields are updated alternately. This representation is subject to the stability criterion $N\delta t < 2$, which can be restrictive due to large N values in thin thermal layers.

We optionally evade this stability criterion by modifying the short wavelength components of the change in temperature, in the layers where $N^2$ is large. Again, this method has already been used successfully in ocean prediction (Reference 36). We used a simpler algorithm in the two dimensional work, where the detailed time dependence was not of primary concern.

## 2.5 THE PRESSURE ALGORITHM

### 2.5.1 Treatment of the Pressure Gradient

The pressure field is determined by the continuity equation and the boundary condition of zero normal flow. We obtain a first approximation to the new velocity field by performing an implicit time step (or iteration) using an initial pressure field obtained by extrapolation from the total pressure field at the two previous time steps.

We then correct the velocity field, so that its divergence is zero and there is no normal flow, by adding the gradient of a correction pressure field. This correction pressure is determined by solving a representation of Poisson's equation.

This pressure algorithm is used in our two-dimensional AGCE models (References 31 through 34). It was used previously in the codes described in References 45 and 46.

### 2.5.2 Solution of Poisson Equation

The pressure equation is solved by using the fast Fourier transform in the $\lambda$ direction and by using ADI iteration with Jordan's optimum parameters in the transverse plane. Convergence is rapid, and this method does not increase computation time unduly. Two Fourier transforms are required at each time step. If significantly better Poisson methods for our application become available, we will use them.

## 2.6 INPUT, OUTPUT, DIAGNOSTICS AND GRAPHICS

The problem, numerical method, and output are defined and controlled using a data page in a standard format. This allows us to use default values for most parameters, and to calculate a sequence of cases in one run.

Resulting fields are output to disc files at regular intervals. This allows us to use separate graphics programs without repeating the calculations, and to split long computations into multiple segments.

Significant diagnostic quantities (maxima, integrals, etc.) are printed out in tabular form every few time steps or iterations. This will allow us to monitor convergence and detect when and where problems occur.

Printer graphics are used for testing and development, to provide rapid display of results. Other more sophisticated forms of graphical display will be developed and used for reporting purposes.

## 2.7 CONVERGENCE AND ACCURACY

We will analyze the accuracy of our steady and time-dependent solutions by repeating some of our computations, using smaller time steps and more mesh intervals. This will provide an accurate measure of convergence.

## 2.8 CODING CONSIDERATIONS AND VECTOR HARDWARE

We intend that this code should be as portable as possible, consistent with reasonable speed. We anticipate use on several different computers, by various NASA employees and contractors. We will therefore write most of the code in FORTRAN 66.

The speed constraint is associated with the vector hardware on modern computers. To make full use of this hardware on the Cyber 205 requires a certain amount of non-standard FORTRAN.

We hope eventually to automate the process of transferring the code from computer to computer. Editor programs will translate the non-standard features from dialect to dialect. We have usd such editors previously to transfer a code between IBM and CDC non-vector computers and the vectorizing Texas Instruments ASC (Reference 44).

## Section 3
## VALIDATION OF THE CODE

### 3.1 SPHERICAL GEOMETRY

Although it will not be possible to validate the three-dimensional code in a spherical geometry until the AGCE apparatus is flown in Spacelab, some limited validation is possible. Our present plans are described in the next two paragraphs.

First, consider the results obtained in the numerical design program for the theoretical AGCE regime diagram (see Section 1.3). If we use the basic states as initial conditions and then insert small-amplitude wave perturbations, we should obtain agreement with the previously derived theoretical regime diagram.

Secondly, the code will be able to treat special spherical cases for which laboratory experiments can be performed and measurements obtained. These include the AGCE apparatus, together with various preliminary test versions, because our code includes the option of terrestrial (axial) gravity. They may also include unstratified spherical flows, with differential rotation producing non-axisymmetric motion.

### 3.2 CYLINDRICAL GEOMETRY

Since the three-dimensional code will be designed with the flexibility for easy conversion to cylindrical geometry, it can be checked against known annulus wave flows (References 28-30).

The annulus experiments have demonstrated that as the parameters (temperature difference and rotation rate) are varied, a steady three-dimensional solution with (for example) four waves can break down, and then evolve in a nonlinear way to a five-wave steady solution. It should be possible to simulate this instability and thus to validate the code.

The annulus experiments have also demonstrated periodic flows (vacillations). First, there is amplitude vacillation, in which a four-wave solution fluctuates between almost axisymmetric surface flow and a strongly asymmetric flow. Secondly, there is wave number vacillation, with the flow cycling in a complex manner between a mainly four-wave structure and a mainly five-wave structure. We would hope to be able to simulate both types of vacillation. Related vacillations are of course a major feature of atmospheric flows.

## Section 4
## OTHER APPLICATIONS

In addition to its value for the AGCE program, the three-dimensional code will have several other applications.

In its cylindrical form, we expect to gain new understanding of significant remaining theoretical problems for the annulus time-dependent flows.

The code could also be modified to study ideas for other future, AGCE-type, Spacelab model experiments, simulating perhaps ocean or mantle flows, or stellar or planetary convection.

The code could be modified to simulate aspects of convection flows in a planetary or stellar interior, within the limits of the Boussinesq approximation.

The Boussinesq approximation could be modified to allow a mean density dependent on the total gravitational potential (the anelastic approximation). This would broaden the range of astrophysical problems to which it could be applied.

## Section 5
## REFERENCES


1. Hide, R., 1958: An experimental study of thermal convection in a rotating liquid. Phil. Trans. Roy. Soc. London, A250, 441-478.

2. Fultz, D., R. R. Long, G. V. Owens, W. Bohan, R. Kaylor and J. Weil, 1959: Studies of thermal convection in a rotating cylinder with some implications for large-scale atmospheric motions. Meteor. Monog., Amer. Meteor. Soc., 104 pp.

3. Fowlis, W. W. and R. Hide, 1965: Thermal convection in a rotating annulus of liquid; Effects of viscosity on the transition between axisymmetric and non-axisymmetric flow regimes. J. Atmos. Sci., 22, 541.

4. Kaiser, J. A. C., 1970: Rotating deep annulus convection, Part 2, Wave instabilities, vertical stratification, and associated theories. Tellus, 22, 275-287.

5. Koschmieder, E. L., 1972: Convection in a rotating laterally-heating annulus. J. Fluid Mech., 51, 637-656.

6. Holton, J. R., 1979: An Introduction to Dynamic Meteororology, (Second Edition). International Geophysics Series, 23, Academic Press, New York, 391 pp.

7. Lorenz, E. N., 1962: Simplified dynamic equations applied to the rotating-basin experiments. J. Atmos. Sci., 19, 39-51.

8. Barcilon, V., 1964: Role of Ekman layers in the stability of the symmetric regime obtained in a rotating annulus. J. Atmos. Sci., 21, 291-299.

9. O'Neil, E. J., 1969: The stability of flows in a differentially heated rotating system with rigid bottom and free top. Stud. Appl. Math., 48, 222-256.

10. Williams, G. P., 1967a: Thermal convection in a rotating fluid annulus: Part 1, The basic axisymmetric flow. J. Atmos. Sci., 24, 144-161.

11. Williams, G. P., 1967b: Thermal convection in a rotating fluid annulus: Part 2, Classes of axisymmetric flow. J. Atmos. Sci., 24, 162-174.

12. Williams, G. P., 1971: Baroclinic annulus waves, J. Fluid Mech., 49, 417-448.

13. Lorenz, E. N., 1967: The nature and theory of the general circulation of the atmosphere. World Meteorological Organization, Monograph No. 218.TP.115., 161 pp.

14. Hide, R. and P. J. Mason, 1975: Sloping convections in a rotating fluid. Advances in Physics, 74, 47-100.

15. Fowlis, W. W. and G. H. Fichtl, 1977: Geophysical Fluid flow Model Experiments in Spherical Geometry. Proceedings of the Third NASA Weather and Climate Program Science Review, NASA Conference Publication 2029, Paper No. 32, pp. 177-181.

16. Fowlis, W. W. and S. Arias, 1978: The Effects of Curvature and Viscosity on Baroclinic Instability - A Two-Layer Model. NASA Technical Paper 1328, 25 pp.

17. Geisler, J. E. and W. W. Fowlis, 1979: Theoretical Regime Diagrams for Thermally Driven Flows in a Beta-Plane Channel. J. Atmos. Sci., 36, 1530-1541.

18. Giere, A. C. and W. W. Fowlis, 1980: Baroclinic Instability with Variable Gravity - A Perturbation Analysis. NASA Technical Paper 1586, 22 pp.

19. Antar, B. N. and W. W. Fowlis, 1980: Eigenvalues of a baroclinic stability problem with Ekman damping, J. Atmos. Sci., 37, 1399-1404.

20. Geisler, J. E. and W. W. Fowlis, Theoretical Regime Diagrams for Thermally Driven Flows in a Beta-Plane Channel in the Presence of Variable Gravity. NASA Technical Memorandum 78316, 18 pp.

21. Giere, A. C. and W. W. Fowlis, 1980: Baroclinic instability with variable static stability - A design study for a spherical atmospheric model experiment. Geophys. Astrophys. Fluid Dynamics, 16, 207-224.

## REFERENCES (continued)


22. Antar, B. N. and W. W. Fowlis, 1981: Baroclinic instability of a rotating Hadley cell. Accepted for publication in the J. Amos. Sci.

23. Giere, A. C. and W. W. Fowlis, 1981: A general solution of the Eady-type equation of baroclinic instability. Accepted for publication in Geophys. Astrophys. Fluid Dynamics.

24. Bowden, M. and H. F. Eden, 1965: Thermal convection in a rotating fluid annulus: temperature, heat flow, and flow field observations in the upper symmetric regime. J. Atmos. Sci., 22, 185-195.

25. Kaiser, J. A. C., 1969: Rotating deep annulus convection, I. Thermal properties of the upper symmetric regime. Tellus, 21, 789-805.

26. Warn-Varnus, A., W. W. Fowlis, S. A. Piacsek and S. M. Lee, 1978: Numerical solutions of laser-Doppler measurements of spin-up. J. Fluid Mech., 85, 609-639.

27. Fowlis, W. W., 1979: Remote optical techniques for liquid flow and temperature measurement for Spacelab experiments. Optical Engineering, 18, 281-286.

28. Riehl, H. and D. Fultz, 1957: Jet stream and long waves in a steady rotating-dishpan experiment: structure of the circulation. Quart. J. R. Met. Soc., 83, 215-231.

29. Kaiser, J. A. C., 1972: Rotating deep annulus convection: The steady high amplitude wave regime - internal thermal fields. Geophys. Fluid Dynam., 4, 159-186.

30. Williams, G. P., 1969: Numerical integrations of the three-dimensional Navier-Stokes equations for incompressible flow. J. Fluid Mech., 37, 727-750.

31. Roberts, G. O., 1981: Axisymmetric AGCE Flows and their Stability. Proceedings of the April, 1981 conference on AGCE in Boulder, CO, NASA Conference Publication 2200, edited by W. W. Fowlis and M. H. Davis.

32. Fowlis, W. W. and Roberts, G. O., 1982: The Numerical Design of a Spherical Baroclinic Experiment for Spacelab Flights. Presented at the International Conference on Computational Methods and Experimental Measurements, Washington, D.C., July 1982.

REFERENCES (continued)


33. Roberts, G. O. and Kopecky, K. J., 1982: Spherical Layer Codes for AGCE. NASA/MSFC FY-82 Atmospheric Processes Research Review; NASA Conference Publication 2259, pp. 181-3.

34. Fowlis, W. W., Roberts, G. O., Kopecky, K. J., Miller, T. L. and Leslie, F. W., 1982: Experimental and Numerical Studies for the AGCE Design. NASA/MSFC FY-82 Atmospheric Processes Research Review; NASA Conference Publication 2259, pp 184-7.

35. Roberts, G. O., J. Laurence Seftor and W. J. Grabowski, 1980: A Sigma Coordinate Ocean Forecasting Computer Code, Part I, Model Differential Equations, Spatial Finite-Difference Representation and Conservation Properties. Report No. SAI-80-957-WA.

36. Roberts, G. O. and J. Laurence Seftor, 1980: A Sigma Coordinate Ocean Forecasting Computer Code, Part II, Temporal Representation. Report No. SAI-80-957-WA.

37. Seftor, J. Laurence and G. O. Roberts, 1980: A Sigma Coordinate Ocean Forecasting Computer Code, Part III, Code Description. Report No. SAI-80-958-WA.

38. Seftor, J. Laurence, 1980: A Sigma Coordinate Ocean Forecasting Computer Code, Part IV, Description of Graphics Capbility. Report No. SAI-81-262-WA.

39. Seftor, J. Laurence and G. O. Roberts, 1980: A Sigma Coordinate Ocean Forecasting Computer Code, Part V, Results. Report No. SAI-81-299-WA.

40. Roberts, G. O. and D. M. Rubenstein, 1980: Shear Effects on Internal Gravity Wave Propagation. Report No. SAI-80-973-WA.

41. Roberts, G. O. and D. M. Rubenstein, 1980: Fine Structure Effects on Internal Wave Generation and Propagation (U). Report No. SAI-81-331-WA (SECRET).

42. Roberts, G. O. and D. M. Rubenstein, 1981: The Computer Code GORWAK for Stratified Flow Computations, Part I, Code Description (U). Report No. SAI-80-292-WA (SECRET).

REFERENCES (continued)


43. Roberts, G. O. and D. M. Rubenstein, 1981: The Computer Code GORWAK for Stratified Flow Computations, Part II, Code Validation Results (U). Report No. SAI-80-293-WA (SECRET).

44. Roberts, G. O. and D. M. Rubenstein, 1981: The Computer Code GORWAK for Stratified Flow Computations, Part III, Users Manual and Code Listings (U). Report No. SAI-80-294-WA (SECRET).

45. Roberts, G. O., S. A. Piacsek and J. Toomre, 1976: Two-Dimensional Numerical Model of the Near-Field flow for an Ocean Thermal Power Plant, Part I. The Theoretical Approach and a Laboratory Simulation. Report No. SAI-76-624-WA.

46. Roberts, G. O., 1978: Two-Dimensional and Axisymmetric Models for the Flow Near an Ocean Thermal Power Plant. Report No. SAI-79-777-WA.

47. Roberts, G. O., 1983: Three-Dimensional AGCE Code, NASA/MSFC Atmospheric Processes Research Review. May, 1982, 2 pp.